



Aalborg Universitet

AALBORG UNIVERSITY
DENMARK

Production of fuel range oxygenates by supercritical hydrothermal liquefaction of lignocellulosic model systems

Pedersen, Thomas Helmer; Rosendahl, Lasse Aistrup

Published in:
Biomass & Bioenergy

DOI (link to publication from Publisher):
[10.1016/j.biombioe.2015.09.014](https://doi.org/10.1016/j.biombioe.2015.09.014)

Creative Commons License
CC BY-NC-ND 4.0

Publication date:
2015

Document Version
Accepted author manuscript, peer reviewed version

[Link to publication from Aalborg University](#)

Citation for published version (APA):
Pedersen, T. H., & Rosendahl, L. A. (2015). Production of fuel range oxygenates by supercritical hydrothermal liquefaction of lignocellulosic model systems. *Biomass & Bioenergy*, 83, 206-215.
<https://doi.org/10.1016/j.biombioe.2015.09.014>

General rights

Copyright and moral rights for the publications made accessible in the public portal are retained by the authors and/or other copyright owners and it is a condition of accessing publications that users recognise and abide by the legal requirements associated with these rights.

- ? Users may download and print one copy of any publication from the public portal for the purpose of private study or research.
- ? You may not further distribute the material or use it for any profit-making activity or commercial gain
- ? You may freely distribute the URL identifying the publication in the public portal ?

Take down policy

If you believe that this document breaches copyright please contact us at vbn@aub.aau.dk providing details, and we will remove access to the work immediately and investigate your claim.

1 Production of fuel range oxygenates by supercritical hydrothermal 2 liquefaction of lignocellulosic model systems

3 Thomas H. Pedersen^a, Lasse A. Rosendahl^{a,*}

4 ^a*Department of Energy Technology, Aalborg University, Pontoppidanstrde 101, 9220 Aalborg Øst*

5 **Abstract**

Lignocellulosic model compounds and aspen wood are processed at supercritical hydrothermal conditions to study and understand feedstock impact on biocrude formation and characteristics. Glucose and xylose demonstrate similar yield of biocrude and biochar, similar biocrude characteristics, and it is hypothesized that reaction mechanisms for the two model compounds are indistinguishable. Glucose and xylose are main sources of substituted cyclopentenones and substantial contributors to oxygenated aromatics mainly in the range of C₆-C₉ number of carbon atoms, and potential, sustainable biogasoline candidates. Lignin yields predominantly aromatic biocrudes having similar C₆-C₉ number of carbon atoms. Model mixtures show good predictability in the distribution of substituted cyclopentenones and oxygenated aromatics, but aspen wood-derived biocrude is more aromatic than predicted by model mixtures. The work extends previous work on the understanding of the chemical mechanisms of lignocellulose liquefaction and the biocrude formation. Potential applications for the biocrudes are identified, where significant sustainability issues for the transport sector can be addressed.

6 *Keywords:* Biofuel, Biocrude, Wood liquefaction, Model compounds, Hydrothermal
7 liquefaction, Reaction mechanism

8 **1. Introduction**

9 Hydrothermal processing of biomass in near-critical water is a viable, scalable and renew-
10 able chemical pathway, utilizing the unique properties of hot-compressed water (HCW), to
11 break down the original macromolecules in biomass and convert their fragments into green
12 synthetic liquid (hydrothermal liquefaction, HTL) [1–4] or gaseous fuels (super critical water
13 gasification, SCWG) [5, 6]. The processing technology has been identified as a promising en-

February 27, 2018

Email addresses: thp@et.aau.dk (Thomas H. Pedersen), *lar@et.aau.dk (Lasse A. Rosendahl)

14 ergy efficient and sustainable carbon-neutral platform for valorisation of biomasses through
15 bio-fuel production [7]. Hydrothermal processing has successfully been demonstrated to
16 convert a broad range of biomasses into four easily separated phases; a gas phase rich in
17 carbon dioxide and combustible gases (*e.g.* H₂ and CH₄), a combustible biochar solid phase,
18 a distinct water-soluble organic phase suitable for fine chemical extraction or synthetic gas
19 production, and a bulk, water-insoluble and oxygen-lean fraction commonly termed biocrude,
20 all which comprise an ideal no waste discharge system. The biocrude is a blend of numerous
21 intermediate chemical compounds spanning a broad range from *e.g.* oxygenated aromatics,
22 heterocyclic compounds to long chain aliphatic backbones mostly dependent on the feedstock
23 composition. The feasibility of the conversion step of various biomasses into biocrudes has
24 already been proven mostly in batch and less so in continuous processing systems [7], and
25 techno-economic assessments recognize HTL as a profitable process for marketable sustain-
26 able liquid fuels, even when followed by a subsequent hydrotreatment step to meet hydro-
27 carbon specs for drop-in applications [8–10]. Several studies have shown that the specific
28 composition of the different types of biomass (wood, grass, vegetable oils, algae etc.) has a
29 major influence on the chemical profile of the biocrude [11–19].

30 Predictability between feedstock composition and biocrude characteristics is still a topic
31 that needs attention [13, 20]. General trends have been observed, such as microalgae result-
32 ing mostly in aliphatic structures, mainly due to the high lipid contents, and lignocelluloses
33 resulting in alkylated cyclopentenones and aromatic structures, the latter expected to origi-
34 nate mainly from lignin conversion. The numerous compounds found in the biocrude and the
35 lack of predictability are considered a significant challenge for technology commercialization.
36 Recently, Carrier et al. investigated the conversion of holocellulose, lignin and α -cellulose ex-
37 tracted from fronds (*Pteris vittata L.*) at sub- and supercritical water conditions, and found
38 that the resulting compounds can be grouped into two main compound pools; one consisting
39 of oxygenated and substituted 5-membered ring structures, such as ketonic cyclopentanes
40 and cyclopentenones (CPs), and one consisting of oxygenated and substituted aromatics (OA)
41 [12, 13]. This is a significant simplification of a highly complex pool of compounds, which
42 further simplifies the identification of downstream applications of the resulting liquids, as
43 these can be characterized by compound families or pools rather than individual compounds.

44 It was further found that the first group of 5-membered derivative compounds originated
45 from the carbohydrates and that the aromatic derivatives originated both from the carbohy-
46 drates and lignin. The compounds obtained consisted mainly of oxygenated paraffins, olefins
47 and aromatics and ranged primarily from the C₅ to C₁₀ number of carbon atoms, and had
48 been identified as promising drop-in gasoline candidates [21]. It was also found that the
49 distribution of 5-membered compounds and aromatics was almost invariant to reaction time
50 but sensitive to reaction temperature and feedstock composition, as mentioned above.

51 Although these observations are indicators of expected product compounds, it is of par-
52 ticular interest to investigate if the distribution of the two primary compound pools can be
53 predicted and produced selectively based on varying the feedstock composition. If this is the
54 case, it provides an opportunity to tailor biocrude composition to the intended downstream
55 purpose by manipulating the feedstock composition.

56 To the best of our knowledge, a comprehensive study investigating lignocellulosics from
57 a single model compound and model mixtures point of view does not exist. The main ob-
58 jective of this study is thus a novel contribution to the understanding of the chemistry of
59 biocrude formation and the quality of such biocrudes from a model compound viewpoint. It
60 is generally accepted that alkaline conditions and high process severity leads to higher quality
61 biocrude, which justifies processing at supercritical conditions compared to subcritical con-
62 ditions [7]. Glucose, xylose and alkali lignin as model compounds for cellulose, hemicellulose
63 and lignin, respectively, and their mixtures are processed in an alkaline supercritical water
64 environment to obtain original information on the formation of green fuel range chemicals.
65 It is envisioned that by studying and understanding the biocrude formation of the individual
66 lignocellulose constituents, unique knowledge can be gained towards understanding the rela-
67 tionship between macro-structures (carbohydrates vs. lignin) on the biocrude formation from
68 real biomass feedstock. In this work, an experimental campaign is carried out to investigate:

- 69 1. The formation and characterization of the water-insoluble compounds obtained when
70 processing aspen wood under alkaline supercritical water conditions.
- 71 2. The formation of biocrude from individual model compounds; glucose, xylose and lignin
72 along with the characterization of the individual biocrudes.
- 73 3. The behavior of sugar derived model compounds to understand the biocrude composi-

74 tion to the chemical properties of the input feed.

75 2. Materials and Methods

76 2.1. Materials

77 Glucose, xylose, lignin (alkali, low sulfonate), sorbitol, xylitol and ethylene glycol (EG)
78 were all purchased from Sigma-Aldrich ($\geq 98\%$). Glycerol (99.5 %) was purchased from
79 Brenntag Nordic A/S. Properties of the aspen wood used are listed in Table 1.

Table 1: ^aUltimate analysis was carried out in a Perkin Elmer 2400 Series II CHNS/O system. ^bFibre composition was determined by the Van Soest method in a FOSS 121 Fibertec unit. ^cAsh content measured by heating a sample to 850 °C and hold isothermally for 2 hours. daf = dry,ash-free. N.D. = Not Detected

^a Ultimate analysis (wt. %, daf.)	
C	50.39 (0.86)
H	6.19 (0.08)
N	0.19 (0.02)
S	N.D.
O (by difference)	43.23 (0.08)
^b Fibre Composition (wt. %, db.)	
Cellulose	63.59 (0.86)
Hemicellulose	7.65 (0.11)
Lignin	22.13 (0.17)
Extractives (by difference)	6.63 (0.01)
^c Ash	0.46 (0.02)

80 2.2. Experimental procedure

81 All experiments were carried out in rapidly heated, 10 mL batch micro-reactors. For
82 each run, the reactor was loaded with 5 g of pre-mixed solutions reaching an estimated final
83 autogenous reaction pressure of circa 300 bars. All mixtures consisted of 20 wt. % input
84 bio-feedstock, for all combinations of model compounds, mixtures hereof or real biomass
85 mixed in demineralized water. K_2CO_3 was added as an alkaline catalyst amounting to 10

86 wt. % of the input bio-feedstock (pH 11.5). The reactor was purged with nitrogen before
 87 heating, and then heated to 400 °C in a pre-heated fluidised sand bath (Techne SBL-2D) for
 88 15 minutes (including the heating period) and finally quenched in water. Typical heating
 89 and cooling rates for the micro-reactors are 250-450 K/min. and >1000 K/min., respectively,
 90 conclusively eliminating any heating and cooling rate effects compared to the time spent at
 91 final reaction conditions.

92
 93 Five mixtures (Mix1-5) of glucose, xylose and lignin were investigated to study qualitative
 94 effects on the biocrudes from different compositions. The compositions of the five mixtures
 95 were chosen in order to frame the composition of a variety of lignocellulosic feedstock obtained
 96 from Demirbas et al. [22]. The compositions of the five mixtures are displayed in Table 2.

Table 2: Composition of the five model compound mixtures investigated. The five mixtures are arranged as four corner and one center point, framing the variety of cellulose, hemicellulose and lignin compositions of lignocellulosic biomass [22].

	Mix1	Mix2	Mix3	Mix4	Mix5
Cellulose/Lignin	1/3	1/3	3	3	8/3
Hemicellulose/Lignin	1/3	3	3	1/3	8/3

97 *2.3. Recovery and analysis of biocrude*

98 After the reactor was cooled to room temperature any overpressure was vented through
 99 a top valve. No further attention was given to the gas phase in this work. As in most
 100 comparable work with micro-reactors, extraction and separation of products from the micro-
 101 reactor was found challenging as some products remained partially emulsified in the aqueous
 102 phase and had to be extracted by an appropriate water-insoluble solvent to obtain stable
 103 and reproducible results. In the adopted procedure, the aqueous phase and easily removable
 104 products were poured out of the reactors and filtered to remove any solids. The emulsified
 105 aqueous phase was then extracted using diethyl ether (DEE) which led to a phase separation.

106 The phase separation lead to two identifiable phases: A top DEE with solubles fraction,
 107 and a bottom aqueous phase. The DEE with solubles fraction was decanted and evaporated
 108 to recover the DEE-solubles. The reactor was then rinsed with acetone and the obtained

109 material filtered. After filtration of the solid phase, the acetone fraction was evaporated (556
110 mbar, 40 °C) to remove the acetone. The leftover product, a mixture of biocrude and residual
111 water, was extracted using DEE and finally the DEE with solubles fraction was evaporated
112 (990 mbar, 40 °C) to recover the biocrude. The total amount of solids was dried overnight
113 before weighing. All experiments were performed in triplicates.

114

115 Qualitative analyses of all biocrude samples were carried out on a Thermo Scientific Trace
116 1300 ISQ GC-MS system, (Length: 15 m., i.d.: 0.25 mm., film: 0.25 μm film, TG-SQC col-
117 umn). Prior to analysis, all samples were diluted in DEE and subjected to the following
118 oven temperature profile; 40 °C was held for 3 minutes, then ramped to 325 °C at 8 °C/min
119 and finally kept at this temperature for 4 minutes. Injector and ion source temperatures
120 were 280 °C, split ratio was 1:20, and flow rate of the carrier gas (helium) was 1.0 mL/min.
121 Compounds were identified by mass spectra comparison with the NIST mass spectral data
122 library. Selectivities of compounds were calculated by peak areas.

123

124 For the most abundant compounds, an index of hydrogen deficiency, Ω , was calculated
125 according to Equation 1, expressing the sum of rings and double bonds, such as C=C and
126 C=O, contained within the chemical structures.

$$\Omega = \frac{2 + 2C - H}{2} \quad (1)$$

127 For single ring structures, which have mostly been observed in the biocrudes, $\Omega-1$ then
128 gives the number of hydrogen molecules needed to be added to that structure in order to
129 obtain the corresponding saturated oxygenated hydrocarbons. This does not necessarily
130 correspond to the number of hydrogen molecules needed to obtain the corresponding alkanes,
131 since the carbonyl groups (C=O), for instance, only represents one double bond but two
132 hydrogen molecules are needed to remove the oxygen. Moreover, an effective hydrogen-to-
133 carbon ratio, H/C_{eff} , was calculated as a quality measure for each compound according to
134 Equation 2.

$$H/C_{\text{eff}} = \frac{H-2O}{C} \quad (2)$$

135 Finally, the boiling point (BP) and the density for each compound are given. For those
136 compounds, of which the boiling points and densities could not be obtained from litera-
137 ture, the Yamamoto-Molecular Break (Y-MB) method is used. The Y-MB method estimates
138 physico-chemical properties by breaking the specific compound SMILES (Simplified Molec-
139 ular Input Line Entry Syntax) notations into corresponding functional groups.

140
141 Functional group identification was done by IR spectroscopy, carried out at room temper-
142 ature on a Thermo Scientific Nicolet 380. Spectrum resolution was 1 cm^{-1} and recorded in
143 the range of $4000\text{-}700\text{ cm}^{-1}$. Elemental composition was measured using a Perkin Elmer 2400
144 Series II CHNS/O system. Due to a combination of small sample sizes, sample sulphur and
145 nitrogen contents close to the detection limit of the equipment and slightly inhomogeneous
146 samples (giving rise to large standard deviations), it was not possible to measure neither sul-
147 phur nor nitrogen in any of the resulting biocrudes. However, as expected for lignocellulose
148 and indicated in Table 1, these can be neglected.

149 **3. Results and Discussion**

150 *3.1. Characterization of water-insoluble compounds obtained from aspen wood*

151 Aspen wood was processed in order to investigate and characterize obtained water-
152 insoluble chemical compounds. Figure 1 shows that approximately 42 % of the aspen wood is
153 converted into a water-insoluble but ether-soluble biocrude, consisting of numerous chemical
154 compounds. The solid yield amounted to approximately 18 %.

155 GC-MS analysis was carried out to study the chemical compounds contained within the
156 biocrude in order to investigate the origin of the compounds presented in Table 3.

157 Firstly, it is observed that for aspen wood the chemical compounds can be grouped into
158 two main groups, cyclopentenones (CP) and oxygenated aromatics (OA), as it was found
159 from processing fronds [12, 13]. Moreover, it is observed that the majority of compounds
160 range from $\text{C}_5\text{-C}_9$, typical for gasoline range hydrocarbons. In order to characterize the
161 different compounds their $\text{H}/\text{C}_{\text{eff}}$ ratios have been plotted against the total chromatogram in
162 Figure 2. It is noted that the CPs generally show higher $\text{H}/\text{C}_{\text{eff}}$ ratios than the OAs, which
163 is consistent with the hydrogen deficiency, Ω , observed in Table 3. The CPs exhibit Ω of 2 or

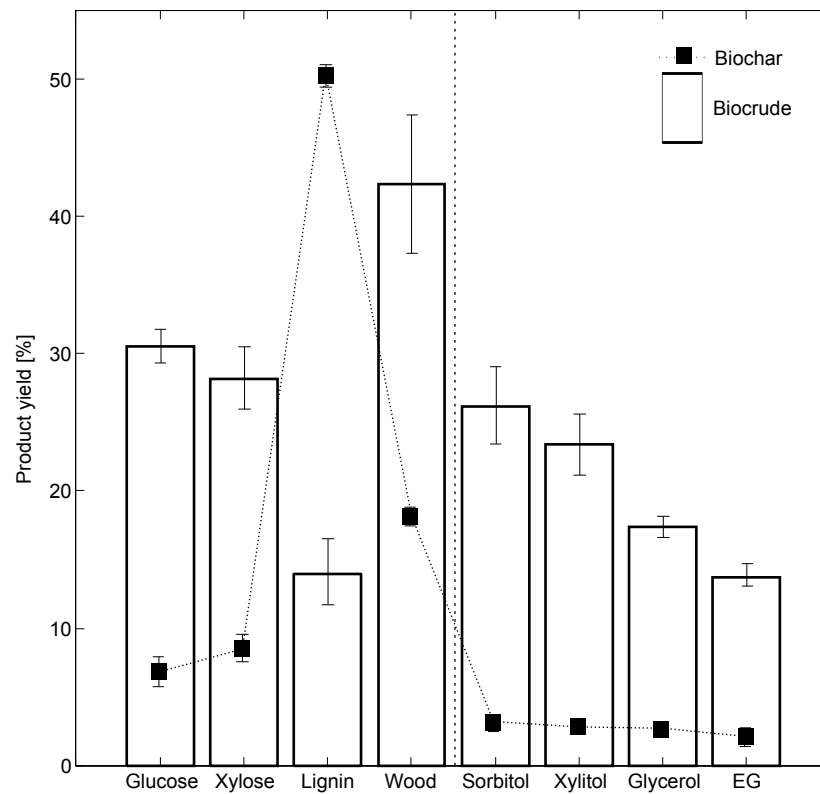


Figure 1: Biocrude and biochar yields for aspen wood, lignocellulosic model compounds and polyols when processed at alkaline conditions at 400 °C and 15 min. EG = Ethylene glycol

Table 3: Main product compounds (by GC-area) obtained when processing aspen wood at alkaline supercritical water conditions. Terminology: (CP), Cyclopentene/pentane derivatives, (OA), Oxygenated aromatics, (HC), Hydrocarbons, (O) Others.

	TR (min)	Compounds	Formula	Ω [-]	H/C _{eff} [-]	BP [°C]	Density [kg/m ³]
1	1.71	Furan, tetrahydro-2,2,5,5-tetramethyl- (O)	C ₈ H ₁₆ O	1	1.75	112	811
2	2.06	Cyclopentanone (CP)	C ₅ H ₈ O	2	1.2	130.6	950
3	2.81	Furan, 2-methyl- (O)	C ₅ H ₆ O	3	0.8	63	927
4	2.94	Cyclopentanone, 2-methyl- (CP)	C ₆ H ₁₀ O	2	1.35	139	917
5	2.99	Diacetone alcohol (CP)	C ₆ H ₁₂ O ₂	1	1.34	166	938
6	4.46	2-Cyclopenten-1-one, 2-methyl- (CP)	C ₆ H ₈ O	3	1.01	154.4	980
7	5.21	1,3-Dimethyl-1-cyclohexene (HC)	C ₈ H ₁₄	0	1.75	128.2	812
8	5.79	2-Cyclopenten-1-one, 3-methyl- (CP)	C ₆ H ₈ O	3	1.01	154.4	980
9	6.32	Phenol (OA)	C ₆ H ₆ O	4	0.67	181.7	1070
10	6.44	2-Cyclopenten-1-one, 3,4-dimethyl- (CP)	C ₇ H ₁₀ O	3	1.15	167.1	952
11	7.39	2-Cyclopenten-1-one, 2,3-dimethyl- (CP)	C ₇ H ₁₀ O	3	1.15	186.9	965
12	7.84	O-Cresol (OA)	C ₇ H ₈ O	4	0.86	191	1047
13	7.92	2-Cyclopenten-1-one, 3,4,4-trimethyl- (CP)	C ₈ H ₁₂ O	3	1.25	182.1	938
14	8.27	p-Cresol (OA)	C ₇ H ₈ O	4	0.86	201.8	1035
15	8.46	Guaiacol (OA)	C ₇ H ₈ O ₂	4	0.56	205	1129
16	8.72	2-Cyclopenten-1-one, 3-(1-methylethyl)- (CP)	C ₈ H ₁₂ O	3	1.25	188.5	934
17	9.66	3,5-Xylenol (OA)	C ₈ H ₁₀ O	4	1	222	981
18	10.5	5-Hydroxy-2,2-dimethylhexan-3-one (O)	C ₈ H ₁₆ O ₂	1	1.5	203	946
19	10.64	Catechol (OA)	C ₆ H ₆ O ₂	4	0.34	245.5	1344
20	11.31	m-Cresol, 5-ethyl- (OA)	C ₉ H ₁₂ O	4	1.11	224	964
21	11.7	p-Cresol, 2-ethyl- (OA)	C ₇ H ₈ O ₂	4	0.56	224	964
22	11.79	Phenol, 2,4,6-trimethyl- (OA)	C ₉ H ₁₂ O	4	1.11	221	984
23	12	4-Ethylguaiacol (OA)	C ₉ H ₁₂ O ₂	4	0.89	235	1041
24	12.22	4-Methylcatechol (OA)	C ₇ H ₈ O ₂	4	0.56	251	1123
25	13.25	1,3-Benzenediol, 4,5-dimethyl- (OA)	C ₈ H ₁₀ O ₂	4	0.75	284.1	1162
26	13.77	4-Ethylcatechol (OA)	C ₈ H ₁₀ O ₂	4	0.75	272.7	1086
27	14.13	1,4-Benzenediol, 2,5-dimethyl- (OA)	C ₈ H ₁₀ O ₂	4	0.75	278.3	1108
28	14.54	1,4-Benzenediol, 2,3,5-trimethyl- (OA)	C ₉ H ₁₂ O ₂	4	0.89	293.8	1100
29	14.72	4-Ethylguaiacol (OA)	C ₉ H ₁₂ O ₂	4	0.89	235	1041
30	15.2	1,3-Benzenediol, 4-propyl- (OA)	C ₉ H ₁₂ O ₂	4	0.89	286	1055
31	15.46	Benzene, 3-ethyl-1,2,4,5-tetramethyl- (HC)	C ₁₂ H ₁₈	4	1.5	231.3	889
32	15.68	Hydroquinone, trimethyl- (OA)	C ₉ H ₁₂ O ₂	4	0.89	293.8	1100
33	16.07	p-Propylguaiacol (OA)	C ₁₀ H ₁₄ O ₂	4	1	262.5	1018
34	24.54	Retene (HC)	C ₁₈ H ₁₈	10	1	379.6	1062

164 3 corresponding to the ketone double bond ($\Omega=2$) and whether the ring is saturated ($\Omega=0$)
 165 or unsaturated ($\Omega=1$), respectively. All the OAs display Ω s of 4, which correspond to the
 166 single benzene rings.

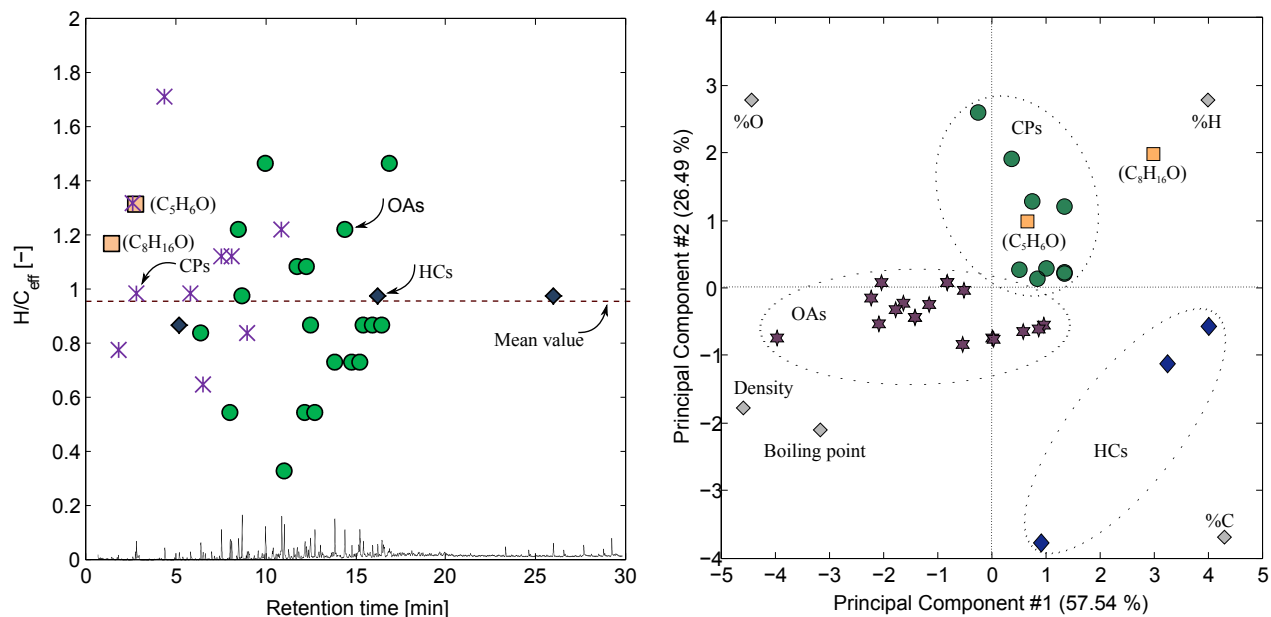


Figure 2: Left: H/C_{eff} for the compounds identified from the aspen wood-derived biocrude. Mean value represented the measured H/C_{eff} of the bulk biocrude from aspen wood. Terminology: (CP), Cyclopentene/pentane derivatives, (OA), Oxygenated aromatics, (HC), Hydrocarbons, (O) Others. Right: Biplot of the PCA model for the compounds identified in the aspen wood-derived biocrude.

167 A principal component analysis (PCA) was further compiled to investigate if the CPs
 168 and the OAs could be further classified based on other parameters than the H/C_{eff} ratio. In
 169 Figure 2 the CPs and the OAs are observed to cluster in two distinct areas indicating simi-
 170 lar characteristics within the clusters but dissimilar characteristics between the two clusters.
 171 Based on the PCA, the CPs generally showed higher hydrogen content and lower oxygen con-
 172 tent than the OAs, which corresponded to the H/C_{eff} ratios. Furthermore, it was recognized
 173 that the OAs showed mostly higher densities and higher boiling points than the CPs. From
 174 an application point of view it is an important fact that the biocrude can be characterized by
 175 two main compound groups with distinct properties, as aromatics and cyclo-olefins/paraffins
 176 are common constituents of transport fuels. As discussed previously, it is of particular in-
 177 terest to investigate if the distribution of the two primary compound pools (OAs and CPs)

178 can be predicted a priori based on the feedstock composition, and subsequently selectively
179 produced according to a specific end use. Therefore, model compound studies were carried
180 out to investigate the formation of biocrude from the individual model compounds (glucose,
181 xylose, and lignin) along with the characterization of the individual biocrudes.

182 *3.2. Characterization of glucose, xylose and lignin derived biocrudes*

183 The conversion of the individual constituents of lignocellulose was investigated at alkali
184 supercritical water conditions. Glucose was selected as an appropriate cellulose model
185 compound, since cellulose readily depolymerises to glucose monomers under the present con-
186 ditions [23]. Xylose was selected as a hemicellulose model compound, since xylan is generally
187 the main constituent for hardwood hemicellulose [24]. As with cellulose, xylan readily de-
188 polymerises to xylose monomers at the given conditions. Alkali lignin (Sigma Aldrich) was
189 chosen as the lignin representative.

190 Figure 1 shows that lignin produced a significantly amount of biochar, around 50 wt.
191 %, and less biocrude, around 15 wt. %, than is the case of glucose and xylose, which is
192 consistent with previous studies [11, 25]. Although it appears that glucose produces slightly
193 more biocrude than xylose (30.6 vs. 28.2 wt. %, respectively), and slightly less biochar (6.9
194 vs. 8.6 wt. %, respectively), taking experimental variations into account, the yield distribu-
195 tion (biocrude and biochar) from glucose and xylose are statistically indifferent based on the
196 Student's t-test. Hence, from the present observations it can be objectively concluded that
197 glucose and xylose give similar yields under the investigated conditions. It also appears, that
198 all model compounds produced less biocrude than that obtained from aspen wood, indicating
199 that synergetic reactions must occur enhancing the biocrude formation. Assuming that the
200 yield can be estimated by a weighted sum of the model compounds, the calculated biocrude
201 mass yield of aspen wood should be approximately 26 %, but 42 % is obtained experimen-
202 tally. Calculated biochar yield of aspen wood is around 16 %, based on model compounds,
203 compared to the 18 % obtained experimentally.

204

205 *Infrared spectroscopy* of the biocrudes was carried out to investigate chemical functional-
206 ities. It is important to keep in mind, that such "qualification" is severely hampered by the
207 complex crude mixtures containing plentiful chemical substances. Therefore, results from

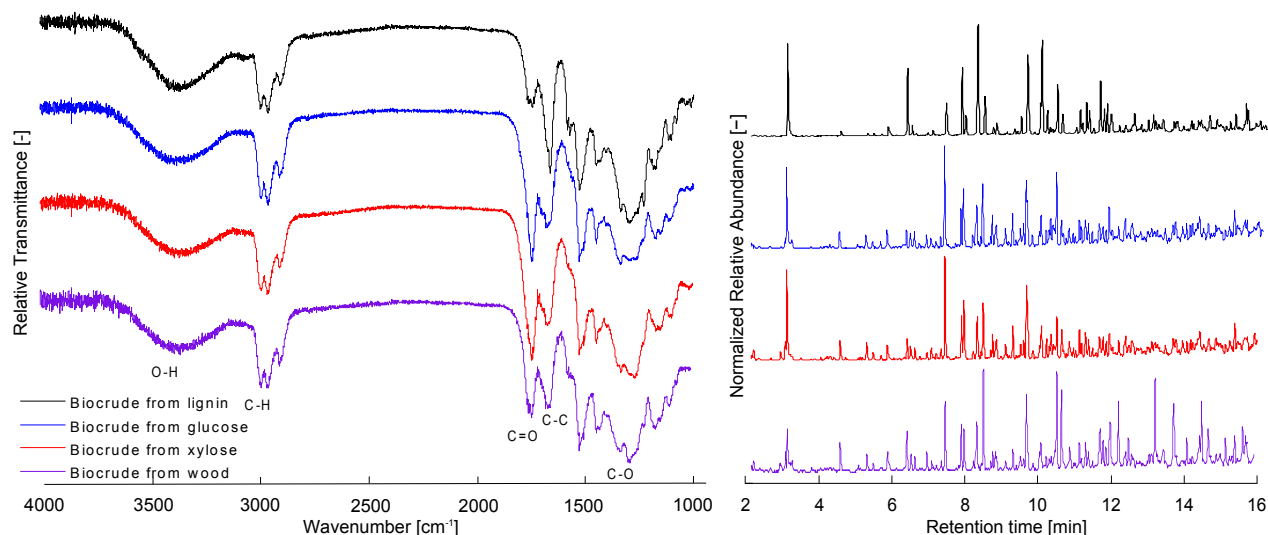


Figure 3: Left: IR spectra of the biocrudes obtained from glucose, xylose, lignin and aspen wood, and Right: Normalized gas chromatography/mass spectroscopy chromatograms.

208 such analysis may not be conclusive but rather used to qualify similarities/differences and
 209 hence distinguish biocrudes obtained from different model compounds and mixtures. In Fig-
 210 ure 3 IR spectra from the glucose, xylose, lignin and aspen wood experiments are shown.
 211 First of all, it is observed that the four biocrudes display similar IR absorption spectra,
 212 which indicates analogous chemical structures. All spectra exhibit pronounced absorptions
 213 in the vicinity of $3650\text{-}3100\text{ cm}^{-1}$, typical for the -OH functional group. Unavoidably, this
 214 absorption is contributed by residual water that is still bound in the biocrude phase, even
 215 though DEE was applied for extraction. Unfortunately, it was not possible to quantify the
 216 amount of residual water by *e.g.* Karl Fisher titration due to small sample sizes. As de-
 217 tected by the mass spectrometry of the biocrude obtained from wood, the -OH absorption
 218 contribution is most likely to be present due to aromatic -OH stretching as phenolic com-
 219 pounds were detected in all biocrudes. The region between $3000\text{-}2800\text{ cm}^{-1}$, typical for C-H
 220 bond absorptions, are observed on all spectra. These absorption contributions are ascribed
 221 to the majority of the cycloalkenes/alkane (CPs) and the aromatic structures (OA and HC)
 222 represented, but also to a minor extent alkyl groups present. The absorptions between 1780
 223 and 1680 cm^{-1} is attributed to C=O bond stretching and is observed to be more intense for
 224 biocrudes obtained from carbohydrates and aspen wood than for the lignin-derived biocrude.

225 This observation is consistent with the observation of cyclic ketones in the biocrude from
226 carbohydrate containing feedstock, which only presents a minor fraction in the lignin-derived
227 biocrude. The region from 1600-1585 cm^{-1} , together with the band in the vicinity of 1500-
228 1400 cm^{-1} and the strong absorption below 900 cm^{-1} in the fingerprint region indicate in-ring
229 C-C bond stretch, interpreted as substituted aromatics. Not surprisingly due to the inher-
230 ent aromatic origin, the absorptions in this region are more intense for the lignin-derived
231 biocrude, than for carbohydrates derived biocrudes. But it is noticeable that, by IR inter-
232 pretation, in terms of aromatic structure, biocrudes obtained from carbohydrates exhibit a
233 similar aromatic structure to that from lignin. In previous studies carbohydrates have only
234 been attributed as a minor source of aromatic structures [26, 27], but present results show a
235 more equalized contribution among the wood constituents. Observed from mass spectrom-
236 etry, the C=C peaks are interpreted to be contributed by oxygenated aromatics and by ketonic
237 cyclopentene/pentane structures. The broad band at 1400-1100 cm^{-1} is attributed to C-O
238 functionalities such as the alcohols, phenols, ethers, and esters observed in all biocrudes.
239 Based on IR interpretation the aspen wood biocrude exhibits more C=O functionalities than
240 the lignin-derived biocrude, and slightly less than the glucose and xylose derived biocrudes.
241 It was observed that IR spectra of biocrudes obtained from any of mixtures (Mix1-5) show
242 similar properties. In fact, by comparing any of the biocrudes from the three model com-
243 pounds and mixtures hereof with the aspen wood or real lignocellulosic biomasses from other
244 studies, it is remarkable how similar the biocrudes are in terms of IR spectroscopy [26, 28].
245 This is further supported by observing the GC-MS spectra of the four biocrudes from the
246 three model compounds and the aspen wood in Figure 3. Although the relative abundances
247 vary for the individual compounds, significant similarities can be identified. It is readily
248 observed that the majority of chemical compounds from both biocrudes are alike, which was
249 also suggested by the IR spectra. In fact, all the compounds identified from the model com-
250 pound biocrudes were traced in the aspen wood-derived biocrude.

251

252 In addition to small organic compounds like propionic acid, propylene glycol and multiple
253 ring compounds, the majority of ether-soluble compounds (>70 %, by GC-area) was found
254 to be CPs and OAs in the C₆-C₉ carbon chain range for the model compound biocrudes,

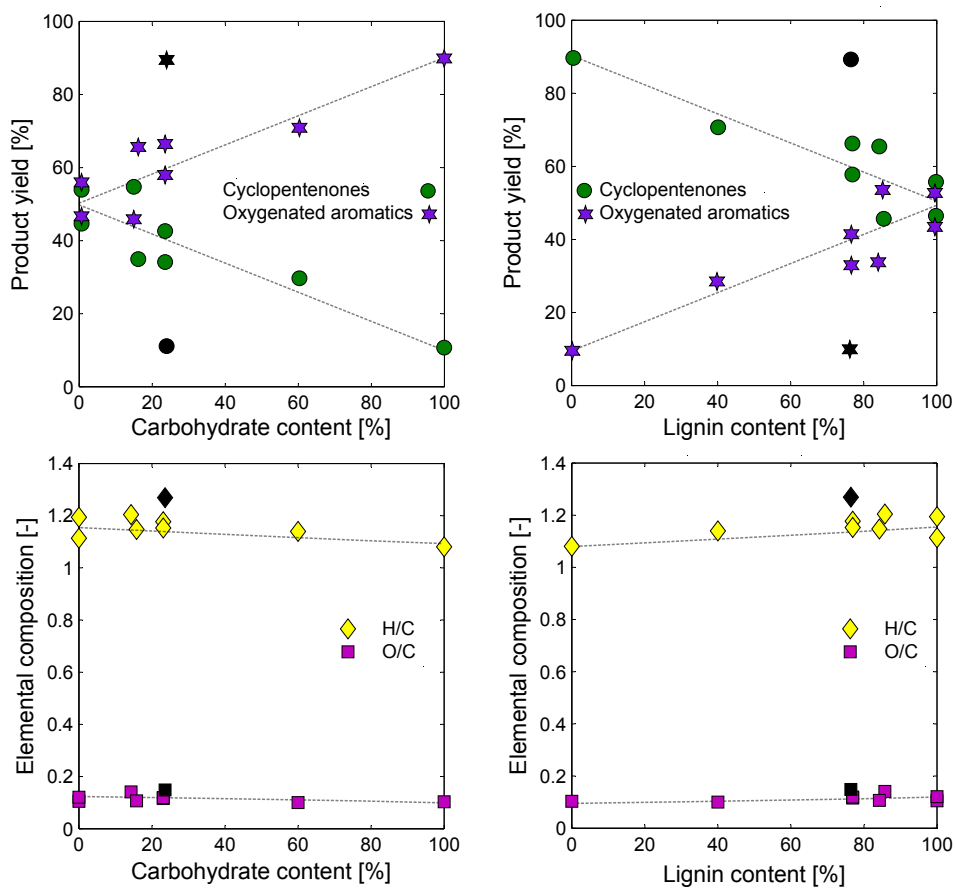


Figure 4: Normalized relative distributions of cyclopentenones (CPs) and oxygenated aromatics (OAs) in the biocrudes, and atomic H/C and O/C ratios as functions of the carbohydrate and lignin content in the model mixtures. Black markers represent the aspen wood-derived biocrude.

255 similar to the observation of the aspen wood-derived biocrude. In order to investigate the
256 effect of feed composition, *i.e.* the relative amount of glucose, xylose and lignin, on the
257 biocrudes composition, Figure 4 shows the normalised distribution of cyclopentenones (CPs)
258 and oxygenated aromatics (OAs) as a function of carbohydrate and lignin content of the
259 model mixtures. It was found that the relative content of aromatics increases according to
260 the sequence: lignin > xylose \approx glucose. Linear trends were found between of amount of CPs
261 and OAs in the biocrudes to the amount of carbohydrates and lignin in the model mixtures.
262 Diverging from this trend is the aspen wood-derived biocrude. In structural composition,
263 Mix4 mimics the aspen wood but it clearly appears that the wood biocrude displays a more
264 distinct aromatic nature and deviating from the linear trends. This fact identifies a poten-
265 tial challenge when model compound mixtures are compared to real biomasses. A plausible
266 explanation for the observed discrepancy between model compound mixtures and the aspen
267 wood may be found the fundamental chemical differences. The alkali lignin used as lignin
268 model compound was found slightly alkaline, when slurried in water (pH 9 in a 20 % dry
269 matter slurry). Conversely, it was found that when slurrying aspen wood in water, acidic
270 conditions were observed (pH 4 in a 20 % dry matter slurry). The pH has a significant
271 influence on the chemical pathway, where alkaline conditions favour Retro-Aldol reactions,
272 whereas acidic conditions favour dehydration of carbohydrates and hence aromatics forma-
273 tion. Furthermore, from a structural point of view it has previously been found that the type
274 of lignin and the crystallinity of cellulose are influential factors on the product distribution
275 [18, 29, 30]. Further investigation on such factors have to be carried out to conclude if this
276 may influence the compound distribution between real biomass and model mixtures.

277

278 *Elemental analyses* of the biocrudes, presented by atomic H/C and O/C ratios, as a
279 function of carbohydrates and lignin content in the feed are shown in Figure 4. Similarity
280 among the obtained biocrudes was previously revealed from the IR measurements, supported
281 by GC-MS identification of structurally identical compounds and is further manifested by
282 the elemental analyses. Interestingly, it was observed that the atomic ratios of the glucose,
283 xylose and lignin-derived biocrudes were equal, which is in agreement with earlier findings
284 [25, 31]. Hence, the H/C and O/C ratios were found almost invariant to the feed composition

285 represented by the zero slope trends in Figure 4. A common denominator for all experiments
286 was that the oxygen contents of all biocrudes were significantly lower than that of the cor-
287 responding starting materials. For glucose and xylose, which are of equal initial H/C and
288 O/C ratios, it was observed that both the H/C and O/C ratios decreased when comparing
289 to the biocrudes, supporting the hypothesis that biocrude compounds were initially formed
290 along a dehydration pathway. The oxygen contents decreased from approximately 53 wt. %
291 to 11.3 (± 0.35) and 12.8 (± 0.42) wt. % for glucose and xylose, respectively. Alkali lignin
292 was also observed to proceed along a similar trajectory, along which both the H/C and O/C
293 ratios decreased, but less pronounced than observed for glucose and xylose. As opposed to
294 glucose and xylose, lignin did not dehydrate but likely liberated oxygen by decarboxylation
295 and/or decarbonylation. The decrease in H/C ratio may also be explained by loss of methyl-
296 and methoxy-groups or due to the fact that alkali lignin probably contained residual polysac-
297 charides, giving rise to a dehydration pathway which was then superimposed on the actually
298 lignin trajectory.

299

300 *TGA-simulated distillation* was performed to estimate the relative distribution of com-
301 pounds based on boiling points. According to Duan et al. the method resembles a miniature
302 distillation evaluating the boiling range of biocrude, although it is likely that some degra-
303 dation at elevated temperatures occur [32]. Hence, the method does not truly yield a true
304 boiling point distribution but enables evaluation of the different biocrudes relatively to each
305 other. Results are presented in Figure 5, which also presents distillation data on commercial
306 fuels and general cuts. Again, it is noted that the biocrudes from glucose and xylose showed
307 identical trends. It was previously mentioned, that the compounds identified in the biocrudes
308 are potential gasoline compounds, showing high octane ratings and good solubility in gasoline
309 [21]. However, from Figure 5 it can be observed that less than 20 % of the total biocrude
310 masses distilled under the boiling point range of marketable gasoline (EN 228). Slightly
311 less than 40 % distilled under the boiling range of diesel (EN 590) and roughly 80 % of the
312 biocrude masses distilled under boiling range of gas oil. Like for the CP/OA distributions,
313 the aspen wood and lignin-derived biocrudes showed comparable TGA curves. Slightly higher
314 than for the glucose and xylose biocrudes, the lignin and aspen wood biocrudes displayed

315 over 60 % of cumulative fractions under the boiling point of common diesel (EN 590). The
 316 cumulative fractions under the boiling point of gas oil are comparable to the glucose and
 317 xylose derived biocrudes. Figure 5 also illustrates the different volatile compounds identified
 318 by GC-MS according to their boiling point reported in Table 3.

319

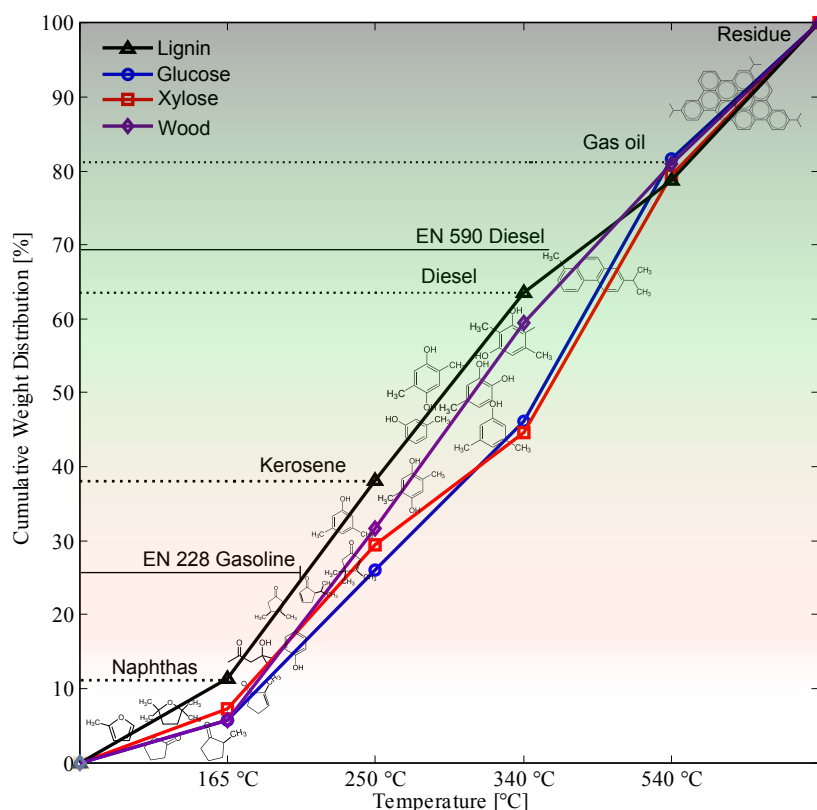


Figure 5: TGA-simulated distillation of the glucose, xylose, lignin and aspen wood-derived biocrudes. True distillation data of commercial fuels and crude oil cuts are included. A pseudo compound is illustrated in the residue temperature range.

320 *The reaction mechanism* is complex and consists of multiple chemical reactions. The ap-
 321 parent similarities between the glucose and xylose biocrudes both in terms of yield, composi-
 322 tion and the chemical analyses performed, suggest that the chemical mechanism is identical
 323 for the two model compounds. This fact significantly reduces the mechanism complexity, and
 324 it is hypothesized that all carbohydrates performed equally and that lignocellulose, in general,
 325 then can be modeled as only carbohydrates and lignin, without considering the distribution
 326 of cellulose and hemicellulose macrostructures.

327 Carbohydrates are known to degrade along two main pathways in hot-compressed wa-
328 ter; dehydration and Retro-Aldol condensation. As previously noticed in other studies, the
329 product compounds observed in the biocrudes, suggest that glucose and xylose follow the
330 dehydration pathway, leading to cyclization of the C₅ (xylose) and C₆ (glucose) structures
331 such as furfural and 5-HMF [4, 19]. At severe conditions furfurals undergo decarbonylation
332 losing oxygen and carbon causing a decrease in carbon chain number, or dehydration leading
333 ultimately to the formation of aromatic compounds (OAs) [33]. Furthermore, the increase in
334 carbon chain numbers to mainly C₅-C₉ compounds then suggests substitution and condensa-
335 tion reactions like Friedel-Crafts, Aldol or Diels-Adler reactions with short chained (C₁-C₄)
336 compounds resulting in ketonization. Retro-Aldol reactions of sugars are known for the pro-
337 duction of such short chained compounds and often found the in water phase, mainly in the
338 form of aldehydes, alcohols and ketones, and greatly promoted by high alkalinity [34].

339 Table 4 shows the time dependent total carbon content (TOC) and the pH of the wa-
340 ter phase when processing glucose, which manifests, that acidic compounds were initially
341 formed, most likely alongside dehydration reactions. The pH was observed to decrease dras-
342 tically from an initially strong alkaline solution to acidic conditions. The pH then slightly
343 increased, indicating consumption of acidic compounds probably through condensation re-
344 actions. Carboxylic acids have been observed to form ketones under the given conditions,
345 which explains the pH decrease and observation of ketones in the biocrude. The observation
346 was accompanied by TOC measurements of the water phase. Initially, the TOC decreased
347 explaining the consumption of short chained C₁-C₄ acidic compounds. The pH and TOC
348 were observed to stabilize with increasing reaction time. Hence, it is hypothesized that glu-
349 cose and xylose degraded into a pool of identical short chained intermediates, which then
350 further recombined and condensed internally or with compounds formed along a dehydration
351 pathway. These reactions, combined with decarboxylation and decarbonylation, are plausible
352 explanations for the increasing carbon chain number and decreasing oxygen content.

353 From the GC-MS spectra in Figure 3 it is noted that the first distinct peak, identified to
354 be diacetone alcohol, was far more pronounced for the model compound biocrudes than for
355 the aspen wood biocrude. It is hypothesized that diacetone alcohol formed *via* condensation
356 of two acetone molecules; acetone, which was known to form from acetic acid condensation.

Table 4: Time course of pH and total organic carbon (TOC) of the water phase during processing of glucose.

	Initial	1 min.	3 min.	5 min.
pH	11.5	4.01	5.05	5.25
TOC [mg/L]	100	53.3	35.3	37.9

357 Acetic acid is known to form *via* Retro-Aldol reactions of carbohydrates, including glucose
 358 and xylose, catalysed by alkaline and supercritical conditions. Again, it must be also kept
 359 in mind that residual polysaccharides are likely to be found in the alkali lignin due to a
 360 non-ideal fractionation, which may explain the presence of diacetone alcohol formed from
 361 carbohydrates. The formation of cyclopentene and cyclopentane derivatives (CPs) is a more
 362 complex mechanism, but it is here proposed that diacetone alcohol cyclization is a plausible
 363 reaction for the formation of the cyclopentane backbone. Substitution and condensation
 364 reactions, hydrogen-transfer reactions etc. may then assist in increasing the number of carbon
 365 atoms of the resulting compounds.

366 Lignin is believed to degrade primarily through cleavage reactions or by hydrolysis of
 367 ether-bonds forming mainly OAs. Decarbonylation or decarboxylation alongside losses of
 368 methyl- and methoxy-groups are plausible side reactions explaining the decrease in observed
 369 H/C ratio. Despite the fact that the chemical pathway to biocrude compounds varies among
 370 lignin and carbohydrates, the elemental composition of the lignin-derived biocrude was found
 371 alike to those obtained from glucose and xylose, but far more aromatic in structure. How-
 372 ever, based only on bulk properties like elemental composition, heating value etc., one will
 373 observe that the properties of biocrudes are practically invariant in terms of the cellulose,
 374 hemicellulose and lignin ratios in the feed. On a more molecular level, one will however
 375 observe that chemical functionalities of the biocrudes change due to its origin; more ketones are
 376 formed from glucose and xylose while aromatic compounds like phenols and catechols etc.
 377 are formed from lignin.

378

379 3.3. Characterization of biocrudes from carbohydrate derived model compounds

380 It was elucidated that carbohydrates, glucose and xylose, form biocrude compounds
 381 through an initial dehydration pathway parallel to Retro-Aldol reactions forming to dis-

382 tinct pools of intermediates. Followed by reductive condensation reactions within or between
383 the intermediates, the carbon chain numbers were observed to increase from the C₅ and C₆
384 of the initial compounds. To investigate if these pathways were common for other similar
385 compounds, four different polyols; sorbitol (C₆), xylitol (C₅), glycerol (C₃) and ethylene gly-
386 col (C₂) were all processed under identical hydrothermal conditions. All compounds yielded
387 equal O/C ratios (O/C=1) but varying H/C ratios. In Figure 1 it is noticed, that all com-
388 pounds formed an ether-soluble phase (biocrudes) and a biochar phase, indicating that even
389 shorter chained polyols, such as glycerol and ethylene glycol, are prone to condensation,
390 likely through Retro-Aldol reactions. In fact, it was found that cyclic compounds are formed
391 similar to those found in the glucose and xylose experiments, supporting the hypothesis that
392 biocrudes were formed *via* an intermediate pool of short-chained compounds.

393 Like for the biocrude elemental composition, it was found that yields were correspondingly
394 affected by the elemental composition of the starting materials. It is realized that for the
395 given model compounds the higher the H/C_{eff} ratio the lower the biocrude and biochar yields.
396 However, the chain number may be a latent factor, since the higher the H/C_{eff} the lower the
397 carbon chain number for the investigated model compounds. Interestingly, the biocrudes
398 obtained from the four polyols showed H/C and O/C ratios equal to those from previous ex-
399 periments. These observations also support the hypothesis, that biocrude compounds from
400 carbohydrates and their derivatives were formed by initial dehydration reactions, followed by
401 condensation/oligomerization reactions increasing the compound carbon chain number and
402 ultimately causing biochar formation.

403
404 Based on the number of carbon atoms observed for the compound majority, the com-
405 pounds obtained suggest gasoline range applications. It was observed that oxygen atoms
406 were mainly positioned in only two oxygen-containing functional groups; ketones (CPs) and
407 alcohols in phenolic compounds (OAs), which deliver valuable information to downstream
408 processes. Important biofuel parameters such as reactivity, solubility in other liquid fuels,
409 combustion properties, vapor pressure etc. are all affected by the compound structures.
410 Naturally, oxygenated functionalities may also cause undesirable properties, *e.g.* increased
411 densities and boiling points, why a subsequent upgrading-processing step, *e.g.* hydrotreat-

412 ment, may be required to meet hydrocarbon drop-in specifications and enhance fuel related
 413 properties such as heating value and volatility etc. Here, hydrogen consumption and equi-
 414 libria of hydrogenation may vary depending on the compound structures, *e.g.* ketonic and
 415 phenolic [24, 35, 36].

416 As expressed previously, Ω can be used as an indicator for the hydrogen required to
 417 convert oxygenates into their corresponding alkanes. Two sample hydrogenation reactions
 418 of two compounds commonly found in the biocrudes are shown in Figure 6. By removing
 419 the oxygen heteroatom in the ketone and phenolic groups and hence converting them into
 420 the corresponding hydrocarbons by hydrodeoxygenation, their properties in terms of heating
 421 value and boiling point are greatly altered. It is observed that by removal of the oxygen
 422 heteroatom, BTX (Benzene, Toluene and Xylene) equivalents are obtained with significantly
 423 higher calorific values and lower boiling points. Secondly, saturation of the compound ring
 424 leads to gasoline equivalents with even higher calorific value and lower boiling point.

425

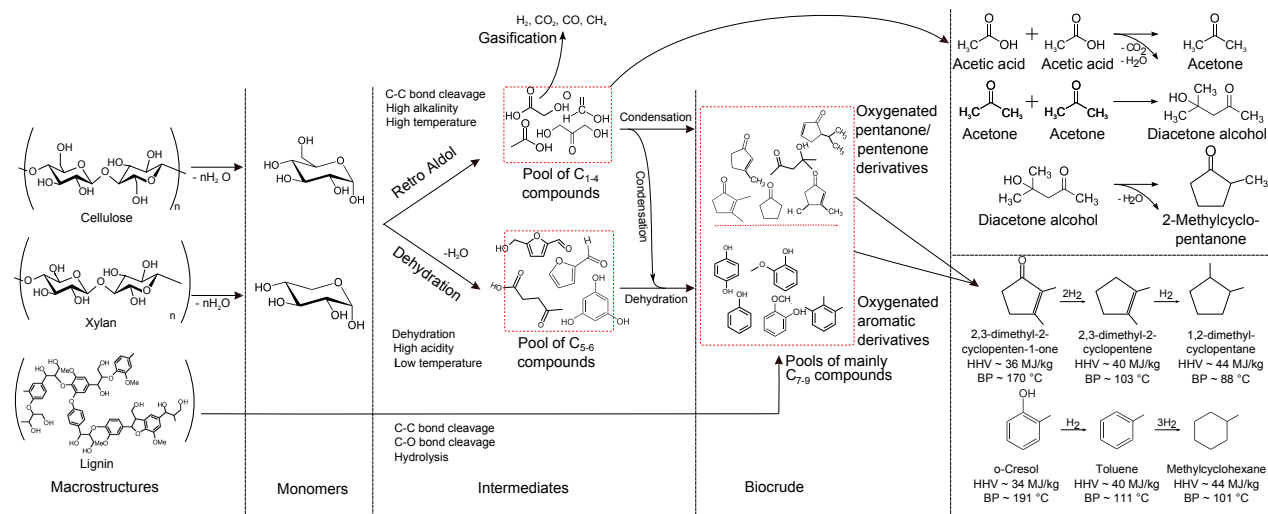


Figure 6: Left: Proposed reaction scheme for the formation of biocrude. Upper right: Proposed reaction for the formation of 2-methylcyclopentanone from acetone. Lower right: Hydrogenation and properties of sample compounds.

426 In conclusion, the biocrudes obtained are potential sources of sustainable biofuels, of
 427 which the properties can be controlled by feedstock composition. However, more work has

428 to be done to understand the lack of predictability between model compounds and real
429 biomasses, and more parametric studies have to be carried out to investigate if the selectivities
430 of cyclopentenones and oxygenated aromatics can be controlled by other process parameters
431 than the feed composition.

432 **4. Conclusions**

433 Compositional effects of lignocellulosic biomass on biocrude formation and characteristics
434 were investigated. The majority of compounds from aspen wood was distributed between two
435 main groups; cyclopentenones and oxygenated aromatics. Based on yields and biocrude char-
436 acteristics, it was concluded that glucose and xylose underwent identical reaction mechanisms.
437 Elemental compositions of the biocrudes were found almost invariant to the distribution of
438 carbohydrates and lignin. Distribution of cyclopentenones and oxygenated aromatics varied
439 linearly to the carbohydrates and lignin contents. Consistency was displayed when comparing
440 model mixtures, however, aspen wood-derived biocrude displayed an inconsistency, in that
441 the biocrude was more aromatic than expected from its analogous model mixture.

442 **Acknowledgements**

443 This work is part of the Flexifuel Project, a Sino-Danish collaboration, and C3BO (Center
444 for BioOil) at the Department of Energy Technology, Aalborg University. The research was
445 financially supported by The Danish Agency for Science, Technology and Innovation (grant
446 no. 10-094552) and The Danish Council for Strategic Research (grant no. 1305-00030B).

447 **References**

- 448 [1] Savage PE, Levine RB, Huelsman CM. Chapter 8 hydrothermal processing of
449 biomass. In: Thermochemical Conversion of Biomass to Liquid Fuels and Chemi-
450 cals. The Royal Society of Chemistry. ISBN 978-1-84973-035-8; 2010, p. 192–221.
451 doi:10.1039/9781849732260-00192.
- 452 [2] Toor SS, Rosendahl L, Rudolf A. Hydrothermal liquefaction of biomass:
453 A review of subcritical water technologies. Energy 2011;36(5):2328 –42.
454 doi:http://dx.doi.org/10.1016/j.energy.2011.03.013.

- 455 [3] Elliott DC. Historical developments in hydroprocessing bio-oils. *Energy & Fuels*
456 2007;21(3):1792–815. doi:10.1021/ef070044u.
- 457 [4] Peterson AA, Vogel F, Lachance RP, Froling M, Antal Jr. MJ, Tester JW. Thermo-
458 chemical biofuel production in hydrothermal media: A review of sub- and supercritical
459 water technologies. *Energy Environ Sci* 2008;1:32–65. doi:10.1039/B810100K.
- 460 [5] Zhou CH, Xia X, Lin CX, Tong DS, Beltramini J. Catalytic conversion of lig-
461 nocellulosic biomass to fine chemicals and fuels. *Chem Soc Rev* 2011;40:5588–617.
462 doi:10.1039/C1CS15124J.
- 463 [6] Demirbas A. Hydrogen production from biomass via supercritical water gasifica-
464 tion. *Energy Sources, Part A: Recovery, Utilization, and Environmental Effects*
465 2010;32(14):1342–54. doi:10.1080/15567030802654038.
- 466 [7] Elliott DC, Biller P, Ross AB, Schmidt AJ, Jones SB. Hydrothermal liquefaction of
467 biomass: Developments from batch to continuous process. *Bioresource Technology*
468 2015;178(0):147–56.
- 469 [8] Huber GW, Iborra S, Corma A. Synthesis of transportation fuels from biomass:
470 Chemistry, catalysts, and engineering. *Chemical Reviews* 2006;106(9):4044–98.
471 doi:10.1021/cr068360d.
- 472 [9] Goudnaan F, van de Beld B, Boerefijn F, Bos G, Naber J, van der Wal S, et al. Thermal
473 Efficiency of the HTU Process for Biomass Liquefaction. Blackwell Science Ltd. ISBN
474 9780470694954; 2008,.
- 475 [10] Tews L, Zhu Y, Drennan C, Elliott D, Snowden-Swan L, Onarheim K, et al. Biomass
476 direct liquefaction options: techno-economic and life cycle assessment. pnnl-23579. Tech.
477 Rep.; Pacific Northwest National Laboratory; 2014.
- 478 [11] Akhtar J, Amin NAS. A review on process conditions for optimum bio-oil yield in
479 hydrothermal liquefaction of biomass. *Renewable and Sustainable Energy Reviews*
480 2011;15(3):1615–24.

- 481 [12] Carrier M, Loppinet-Serani A, Absalon C, Marias F, Aymonier C, Mench M. Conversion
482 of fern (*pteris vittata* L.) biomass from a phytoremediation trial in sub- and supercritical
483 water conditions. *Biomass and Bioenergy* 2011;35(2):872 –83.
- 484 [13] Carrier M, Loppinet-Serani A, Absalon C, Aymonier C, Mench M. Degradation pathways
485 of holocellulose, lignin and α -cellulose from *pteris vittata* fronds in sub- and super critical
486 conditions. *Biomass and Bioenergy* 2012;43(0):65 – 71.
- 487 [14] Xiu S, Shahbazi A. Bio-oil production and upgrading research: A re-
488 view. *Renewable and Sustainable Energy Reviews* 2012;16(7):4406 –14.
489 doi:http://dx.doi.org/10.1016/j.rser.2012.04.028.
- 490 [15] Vardon DR, Sharma B, Scott J, Yu G, Wang Z, Schideman L, et al. Chemical properties
491 of biocrude oil from the hydrothermal liquefaction of spirulina algae, swine manure, and
492 digested anaerobic sludge. *Bioresource Technology* 2011;102(17):8295 –303.
- 493 [16] Jin B, Duan P, Xu Y, Wang F, Fan Y. Co-liquefaction of micro- and macroalgae in
494 subcritical water. *Bioresource Technology* 2013;149(0):103 –10.
- 495 [17] Klingler D, Vogel H. Influence of process parameters on the hydrothermal decomposition
496 and oxidation of glucose in sub- and supercritical water. *The Journal of Supercritical
497 Fluids* 2010;55(1):259 –70.
- 498 [18] Møller M, Harnisch F, Schröder U. Hydrothermal liquefaction of cellulose in subcritical
499 water-the role of crystallinity on the cellulose reactivity. *RSC Adv* 2013;3:11035–44.
500 doi:10.1039/C3RA41582A.
- 501 [19] Aida TM, Shiraishi N, Kubo M, Watanabe M, Jr. RLS. Reaction kinetics of d-xylose in
502 sub- and supercritical water. *The Journal of Supercritical Fluids* 2010;55(1):208 –16.
- 503 [20] Leow S, Witter JR, Vardon DR, Sharma BK, Guest J, Strathmann TJ. Prediction of
504 microalgae hydrothermal liquefaction products from feedstock biochemical composition.
505 *Green Chem* 2015;;–doi:10.1039/C5GC00574D.

- 506 [21] McCormick RL, Ratcliff MA, Christensen E, Fouts L, Luecke J, Chupka GM, et al.
507 Properties of oxygenates found in upgraded biomass pyrolysis oil as components of
508 spark and compression ignition engine fuels. *Energy & Fuels* 2015;29(4):2453–61.
509 doi:10.1021/ef502893g.
- 510 [22] Demirbas A. Relationships between lignin contents and heating values of biomass. *En-
511 ergy Conversion and Management* 2001;42(2):183 –8.
- 512 [23] Sasaki M, Adschiri T, Arai K. Kinetics of cellulose conversion at 25 mpa in sub- and
513 supercritical water. *AIChE Journal* 2004;50(1).
- 514 [24] Hoffmann J, Pedersen T, Rosendahl L. Near-critical and supercritical water and their
515 applications for biorefineries; chap. *Hydrothermal Conversion in Near-Critical Water A
516 Sustainable Way of Producing Renewable Fuels*. Springer Netherlands. ISBN 978-94-
517 017-8922-6; 2008, p. 373–400. doi:10.1007/978-94-017-8923-3.
- 518 [25] Yong TLK, Matsumura Y. Reaction kinetics of the lignin conversion in super-
519 critical water. *Industrial & Engineering Chemistry Research* 2012;51(37):11975–88.
520 doi:10.1021/ie300921d.
- 521 [26] Zhu Z, Rosendahl L, Toor SS, Yu D, Chen G. Hydrothermal liquefaction of barley
522 straw to bio-crude oil: Effects of reaction temperature and aqueous phase recirculation.
523 *Applied Energy* 2015;137(0):183 –92.
- 524 [27] Ohra-aho T, Tenkanen M, Tamminen T. Direct analysis of lignin and lignin-like com-
525 ponents from softwood kraft pulp by py-gc/ms techniques. *Journal of Analytical and
526 Applied Pyrolysis* 2005;74(12):123 –8.
- 527 [28] Cheng S, Dacruz I, Wang M, Leitch M, Xu CC. Highly efficient liquefaction of woody
528 biomass in hot-compressed alcoholwater co-solvents. *Energy & Fuels* 2010;24(9):4659–67.
529 doi:10.1021/ef901218w.
- 530 [29] Yoshida T, Oshima Y, Matsumura Y. Gasification of biomass model compounds and
531 real biomass in supercritical water. *Biomass and Bioenergy* 2004;26(1):71 –8.

- 532 [30] Yanik J, Ebale S, Kruse A, Saglam M, Yuksel M. Biomass gasification in supercritical
533 water: Part 1. effect of the nature of biomass. Fuel 2007;86(15):2410–5.
- 534 [31] Xu C, Lad N. Production of heavy oils with high caloric values by direct liquefac-
535 tion of woody biomass in sub/near-critical water. Energy & Fuels 2008;22(1):635–42.
536 doi:10.1021/ef700424k.
- 537 [32] Duan P, Xu Y, Bai X. Upgrading of crude duckweed bio-oil in subcritical water.
538 Energy & Fuels 2013;27(8):4729–38. URL: <http://dx.doi.org/10.1021/ef4009168>.
539 doi:10.1021/ef4009168. arXiv:<http://dx.doi.org/10.1021/ef4009168>.
- 540 [33] Carlson T, Jae J, Huber G. Mechanistic insights from isotopic
541 studies of glucose conversion to aromatics over zsm-5. ChemCatChem
542 2009;1(1):107–10.
- 543 [34] Yin S, Tan Z. Hydrothermal liquefaction of cellulose to bio-oil under
544 acidic, neutral and alkaline conditions. Applied Energy 2012;92(0):234
545 --9.
- 546 [35] Mortensen P, Grunwaldt JD, Jensen P, Knudsen K, Jensen A. A review of
547 catalytic upgrading of bio-oil to engine fuels. Applied Catalysis A:
548 General 2011;407(12):1 -- 19.
- 549 [36] Furimsky E. Catalytic hydrodeoxygenation. Applied Catalysis A: General
550 2000;199(2):147 --90.